

## OPTICAL BIOPSY IN HUMAN UROLOGIC TISSUE USING OPTICAL COHERENCE TOMOGRAPHY

G. J. TEARNEY,\* M. E. BREZINSKI, J. F. SOUTHERN, B. E. BOUMA, S. A. BOPPART AND  
J. G. FUJIMOTO

*From the Department of Electrical Engineering and Computer Science and Research Laboratory of Electronics, Massachusetts Institute of Technology, Cambridge, Massachusetts, and Massachusetts General Hospital, Boston, Massachusetts*

### ABSTRACT

Optical Coherence Tomography (OCT) is a recently developed non-invasive technique for obtaining high resolution, cross-sectional images of human tissue. This work investigated the capability of OCT to differentiate the architectural morphology of urologic tissue with the long term aim of using OCT as an adjunct to endoscopic imaging and to improve the efficiency of interventional procedures such as transurethral prostatectomy (TURP). Urologic tissues were taken postmortem, dissected, and imaged using OCT. Microstructure was delineated in different urologic tissues, including the prostatic urethra, prostate, bladder, and ureter, with an axial resolution of  $16 \pm 1 \mu\text{m}$ ., higher than any clinically available endoscopic intraluminal imaging technology. The ability of OCT to provide non-contact high resolution imaging of urologic tissue architectural morphology (i.e. optical biopsy), without the need for excisional biopsy, suggests the potential of using OCT to obtain information on tissue microstructure that could only previously be obtained with conventional biopsy.

KEY WORDS: optics, endoluminal, urology, imaging, transurethral prostatectomy

The introduction of endoscopic transluminal imaging has led to substantial reductions in the morbidity and mortality associated with disorders of the urinary tract. However, endoscopic imaging is frequently limited by the relatively low resolution and the inability to access the structure of tissue below the luminal surface. A technology able to obtain "optical biopsies", or high resolution, cross-sectional images of tissue, could substantially improve the diagnosis and treatment of urinary tract disorders. For example, the relatively high occurrence of impotence following transurethral prostatectomy (TURP) would likely benefit from the introduction of high resolution subsurface imaging. It is well documented that the incidence of post-surgical erectile dysfunction and impotence is directly related to perforation of the prostatic capsule and damage to the neurovascular bundles.<sup>1</sup> An imaging technology which can yield resolution in the micron range can potentially provide information on tissue microstructure that would enable localization of the capsule and aid in preventing damage to the neurovascular bundles. In this paper, we introduce optical coherence tomography (OCT) for obtaining non-excisional, high resolution, cross-sectional images of the urinary tract.<sup>2</sup>

OCT is similar to B-mode ultrasound imaging except that it measures reflected infrared light rather than acoustical waves. The intensity of backreflected light from structures within tissue is displayed as a function of depth. Tomographic images are produced by scanning the optical beam across the sample and generating two-dimensional data. Thus, an OCT image represents a cross-sectional depiction of the optical reflectance properties within tissue.<sup>2</sup>

OCT was initially introduced to image the transparent tissue of the eye with an axial resolution of  $10 \mu\text{m}$  and is currently being used in clinical trials to diagnose retinal macular disease.<sup>3,4</sup> Although application of OCT in tissues

which are non-transparent and scatter light is more challenging, preliminary in vitro studies suggest the feasibility for diagnostic imaging in a wide range of tissues.<sup>5-7</sup> OCT is especially promising for imaging atherosclerotic plaque morphology in coronary artery disease.<sup>8</sup> Although the imaging depth of OCT in scattering tissues is limited to a few millimeters, the resolution of this optical technology is approximately 10 times higher than clinical high frequency ultrasound, the currently available technology with the highest resolution for cross-sectional endoluminal imaging.

In addition to high resolution, several features of OCT make it well-suited for intraluminal diagnostics. Because OCT is based on technology used in optical communication, OCT can be constructed with common optical fiber components and integrated with conventional endoscopes. Therefore, OCT imaging can be performed at sites within the urinary tract through optical fibers without the need for a distal transducer. Unlike MRI or CT, OCT is compact and portable. Finally, OCT does not require contact during imaging and can be performed directly through air without the need for a transducing medium.

The purpose of this study is to investigate the capability of OCT to image in vitro microstructure of the urinary tract, with the focus on a critical region consisting of the prostatic capsule, surrounding adipose tissue, and neurovascular bundles. The results of this study will suggest the feasibility of using OCT for high resolution imaging of the urinary tract and serve as a foundation for future in vivo investigations.

### MATERIALS AND METHODS

OCT is analogous to ultrasound B-mode imaging except that it uses infrared light as opposed to acoustical radiation to perform micron resolution ranging and imaging.<sup>2</sup> Ultrasound imaging is accomplished by measuring the delay time (echo delay) for an incident ultrasonic pulse to be reflected back from structures within tissue. Because the velocity of sound is relatively slow, this delay time can be measured electronically. However, since the speed of light is  $10^6$  times higher than sound, OCT measurements of delay time cannot

Accepted for publication December 3, 1996.

\* Requests for reprints: Massachusetts Institute of Technology, Building 36-357, 50 Vassar Street, Cambridge MA 02139.

Supported by NIH grant 9-RO1-EY11289-10 and the Medical Free Electron Laser Program, Office of Naval Research Contract N00014-94-0717.

be performed directly by electronics. Therefore, a correlation technique known as low coherence interferometry is used.

Figure 1 shows a schematic of the OCT system which is based on a fiber optic implementation of a Michelson type interferometer.<sup>2</sup> In a Michelson interferometer, an optical source is incident on a beam splitter. Half of the light emerging from the splitter is directed toward a moving mirror. This light path is known as the reference arm of the interferometer. The remaining light is directed toward the sample. When light reflected from the reference arm is combined with light that has returned from the sample arm, these two beams interfere if the optical path lengths of the two beams are matched to within the coherence length of the light.

The property of light known as the coherence length is analogous to the pulse duration for the measurement of echo delay time. Thus, the coherence length defines the axial resolution of the OCT system. Since interference is detected only when the optical path lengths of the sample and reference arms match to within the coherence length of the source, precision time and distance measurements are possible if the source has a short coherence length. The coherence length is inversely proportional to the width of the optical spectrum (wavelength distribution) of the source.<sup>9</sup> Since the axial resolution of OCT depends only on the coherence properties of the light and not on the focusing parameters, higher axial resolution may be achieved using shorter coherence length light sources. Recent studies have achieved imaging with axial resolution of less than  $4 \mu\text{m}$  using short coherence length sources based on solid state short pulse lasers.<sup>10,11</sup>

The amplitude of reflected light as a function of depth within tissue is obtained by moving the reference arm at a constant velocity (fig. 1) and digitizing the magnitude of the interference pattern. The result is the measurement of optical backscatter or reflectance versus axial range and is somewhat analogous to ultrasound A mode ranging. A cross-sectional image is produced by recording sequential axial reflectance profiles while the beam position is scanned across the sample. The OCT images in this study were acquired by placing the sample on a computer controlled scanning stage, translating the stage, and acquiring axial reflectance profiles for each scan position. For in vivo imaging, the sample will be scanned circumferentially, using a fiber optic endoscope

placed inside the organ lumen. The endoscope to be used for performing intraluminal OCT imaging of in vivo urologic tissues will be similar in design to a recently developed OCT intravascular imaging catheter.<sup>12</sup>

The dimensions of the OCT images acquired in this study were  $3$  (axial)  $\times$   $6$  (transverse) mm which corresponded to an image size of  $250$  (axial)  $\times$   $500$  (transverse) pixels. The image acquisition time was 45 seconds. Future modifications requiring straightforward, albeit time consuming, engineering should achieve image acquisition times at least two orders of magnitude faster than demonstrated in this preliminary study. A prototype system has been recently developed with image acquisition times below one second.<sup>13</sup>

The OCT system used in this experiment is implemented by coupling a superluminescent diode (SLD) with a center wavelength of  $1300 \text{ nm}$ . and a spectral bandwidth of  $50 \text{ nm}$ . into a single-mode fiber optic Michelson interferometer (fig. 1). The OCT system had a free space axial resolution ( $z$ ) of  $16 \pm 1 \mu\text{m}$ . which was determined by measuring the point spread function from a mirror.<sup>8</sup> The transverse resolutions ( $x$  and  $y$ ), determined by the spot size of the focused beam incident on the sample, were measured to be  $25 \mu\text{m}$ . The spot size was chosen so that the transverse resolution was comparable to the axial OCT resolution, while maintaining an appropriate depth of focus (approximately  $1 \text{ mm}$ .). The power incident on the sample was  $150 \mu\text{W}$  which provided a signal to noise ratio (SNR) of  $110 \text{ dB}$ . The SNR is a measure of the minimum detectable reflectance and was empirically determined by comparing the signal from a 100% reflector (mirror) to the variance of the signal with the sample arm blocked. This sample arm power is below the hazardous level for tissue, as determined by the American National Standards Institute (ANSI).<sup>14</sup>

Normal urologic tissue including the prostatic urethra, prostate, bladder, and ureters were obtained within 5 hours of the initiation of autopsy. More than 20 different samples from 5 patients were examined. The tissue samples were placed in isotonic saline with 0.05% Sodium Azide and stored at  $0\text{C}$ . The tissues were dissected to dimensions of approximately  $10 \text{ mm.} \times 5 \text{ mm.}$  and imaged with the luminal surfaces exposed. During imaging, the tissues were partially immersed in isotonic saline to prevent dehydration.

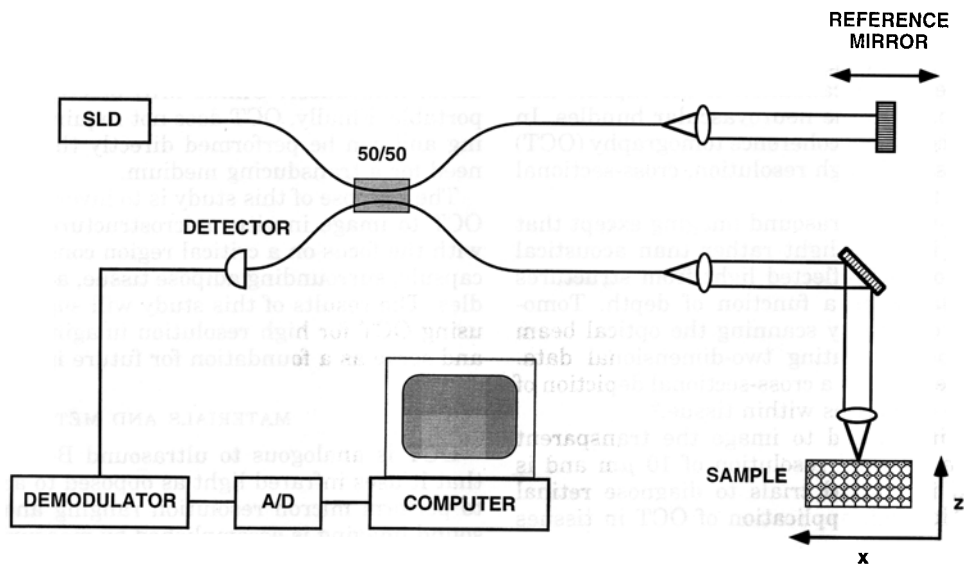


FIG. 1. Schematic of OCT system. Short coherence length superluminescent diode (SLD) is coupled into fiber optic Michelson interferometer. SLD has center wavelength of  $1300 \text{ nm}$ . and spectral bandwidth of  $50 \text{ nm}$ . Half of the light is directed toward reference arm while the other half is directed toward sample. Interference is detected only if reference and sample arm path lengths are matched to within coherence length of the light. Reflectance as function of depth,  $z$ , is obtained by scanning reference arm path length and digitizing the magnitude of demodulated interference. An OCT image is created by acquiring reflectance as a function of depth while scanning the sample arm beam across specimen.

Imaging was performed through air at room temperature. The position of the beam on the sample was monitored using a visible-light guiding beam (633 nm, Helium Neon laser) that was coincident with the 1300 nm, infrared OCT beam on the sample. The imaging planes were marked using small injections of dye. The samples then underwent routine histologic processing. Samples were immersed in 10% buffered formalin for 48 hours. The tissues were then processed for standard paraffin embedding. Five micron thick sections were cut at the marked imaging sites and stained with hematoxylin and eosin (H&E). The stained histologic sections enabled verification of the microstructure of the different samples and allowed identification of sources of tissue contrast in the OCT images.

## RESULTS

**Prostatic urethra.** OCT enables visualization of the architectural microstructure of the prostatic urethra and the periurethral prostate (figs. 2 and 3). Differentiation between the prostatic urethra and the prostate is possible due to the different backreflection characteristics of the two tissue types. Paraurethral gland ducts can be visualized within the urethra (fig. 3). Prostatic glands can be identified in both images (figs. 2 and 3) and demonstrate the capability to image completely through the urethra to the prostate. Areas of relatively low backscatter within the prostatic glands represent the presence of prostatic secretions. Since the resolution of the OCT system used in this study was  $16\ \mu\text{m}$ , the epithelium of the urethra is not resolved.

**Neurovascular bundle.** The high resolution of OCT allows imaging of neurovascular bundles near the capsule at the prostate-adipose tissue border. In fig. 4, a portion of the prostate has been excised and imaged. The prostate tissue appears relatively homogenous at this resolution. The outlines of entire adipose cells can be visualized in this OCT image. A neurovascular bundle can be seen within the adipose tissue adjacent to the prostate (fig. 4). Neurovascular bundles appear to have a high backreflection intensity relative to that of the surrounding adipose tissue. Thus, OCT provides high contrast between neurovascular bundles and adipose tissue at the prostate-adipose border.

**Prostatic capsule.** OCT images of the exterior surface of the prostate demonstrate the capability of OCT to resolve and locate the prostatic capsule (fig. 5). Differentiation of the collagenous layers of the capsule is made possible by the differences in backreflection between the capsule and the prostate. The axial thickness of the capsule in this image can be measured from the OCT image and is approximately  $50\ \mu\text{m}$ . Fig. 5 also shows an artery below the fibrous capsule. Microstructure visible within the artery include the intima and media of the vessel.

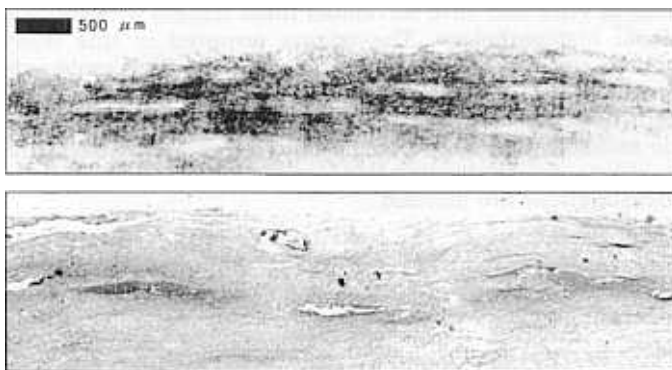


FIG. 2. OCT image of in vitro human prostatic urethra and periurethral prostate and corresponding histology (H&E). Paraurethral glands can be clearly visualized below urethra.

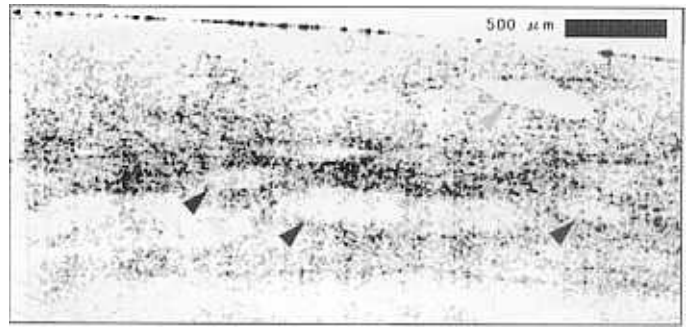


FIG. 3. OCT image of in vitro human prostatic urethra and periurethral prostate. Green arrow points to periurethral gland duct in urethra. Red arrows indicate prostatic glands containing secretions.

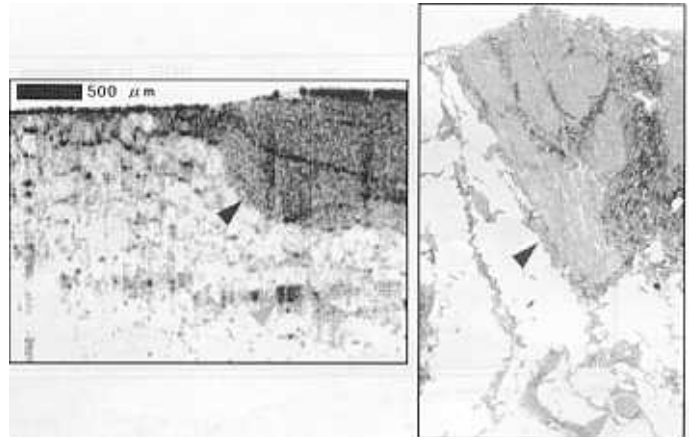


FIG. 4. OCT image of in vitro human prostate-adipose border and histology (H&E). Entire outlines of adipose cells may be seen. Red arrow demarcates prostate-adipose border. Blue arrow points to neurovascular bundle.

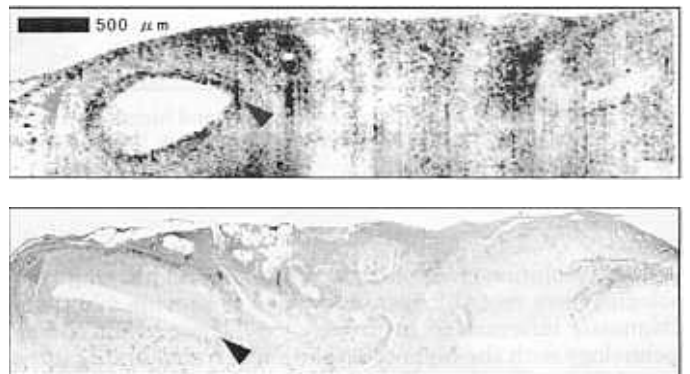


FIG. 5. In vitro prostatic capsule and corresponding histology (H&E). Green arrow points to fibrous prostatic capsule. Microstructure such as border between intima and media of artery can be seen below capsule (red arrow).

**Bladder and ureter.** Different anatomic layers in the bladder can be identified in the OCT image, including the mucosa, submucosa, and muscularis propria (fig. 6). OCT images of the ureter demonstrate the capability of OCT to resolve the mucosa, muscular layers, and adventitia (fig. 7). Differentiation of the mucosa, muscular and adventitial layers is made possible by visualization of the different backreflection characteristics within each layer. The muscular layers seem to have a higher and more regular backreflection intensity than either the mucosal or adventitial layers.



FIG. 6. In vitro human bladder wall and histology (H&E). Borders between mucosa (m), submucosa (sm), and muscularis propria (mp) can be clearly resolved in OCT image.

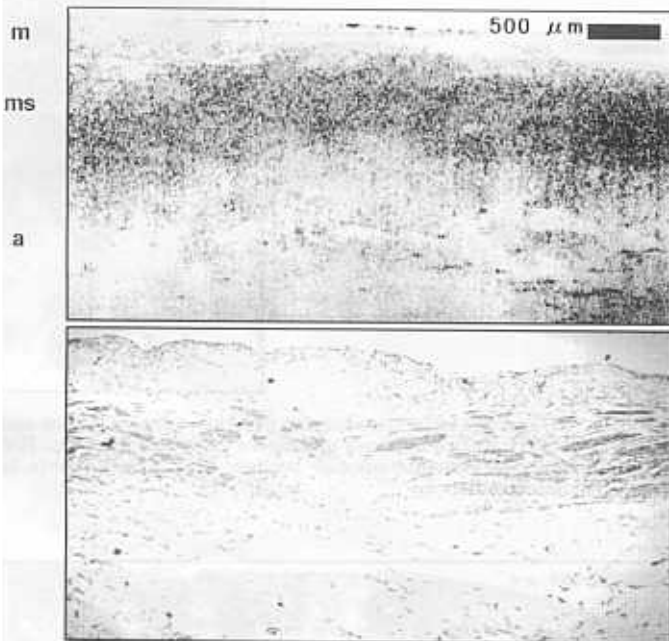


FIG. 7. OCT image of in vitro human ureter and histology (H&E). High degree of contrast is visible between mucosa (m), muscular (ms), and adventitial layers (a).

#### DISCUSSION

High resolution cross-sectional endoluminal imaging technologies have recently been developed to provide additional diagnostic information in urology.<sup>15-19</sup> The current clinical technology with the highest resolution is transluminal ultrasound. This technology uses small high frequency ultrasound transducers (10-20 MHz) to generate axial resolutions in the range of 100  $\mu\text{m}$ . A cross-sectional ultrasonic image is typically produced by rotating the transducer 360 degrees. Imaging of the urologic tissues is performed by filling the lumen with sterile water to couple the ultrasonic probe to the tissue surface. High frequency endoluminal ultrasound has been reported to be useful for evaluating urethral diverticula, the urethral sphincter, staging ureteral and bladder carcinoma, and quantifying the dimensions and location of ureteral calculi.<sup>15-19</sup> However, since axial resolution below 100  $\mu\text{m}$  cannot be achieved, microstructure within tissue layers and cellular structure are poorly differentiated.

OCT has the potential to allow the urologist to delineate tissue microstructure at an axial resolution up to 25 $\times$  higher (4 to 20  $\mu\text{m}$ .) than high frequency ultrasound. In this work, the ability of OCT to resolve tissue morphology was demon-

strated with a 1300 nm. diode source which provided an axial resolution of 16  $\mu\text{m}$ . The feasibility of using OCT for high resolution urologic imaging was suggested by studies performed on representative tissues of the urinary tract. Microstructural details such periurethral exocrine ducts, prostatic glandular secretions, and ureteral muscular layers could be easily identified.

A role for OCT in guiding the resection of hyperplastic prostatic parenchyma has also been suggested. OCT images, with an axial resolution of 16  $\mu\text{m}$ ., sharply delineate the prostate-capsule border. Furthermore, neurovascular bundles can be identified in close approximation to the prostatic capsule. Since postoperative impotence and incontinence have been linked to traumatic transection of these neurovascular bundles, OCT guidance may substantially reduce the morbidity associated with mechanical interventions.

Several issues will need to be addressed before the clinical effectiveness of OCT can be assessed, including improvements in data acquisition rates and incorporation of this technology into a small diameter (2-3 mm.) catheter. The current acquisition times of 45 seconds are not sufficient for in vivo imaging. However, recent improvements in mechanical scanning design and higher power light sources have led to an increase in acquisition rate of almost two orders of magnitude.<sup>20</sup> Further modifications should achieve real time video frame rates. Since OCT is based on technology used in fiber optic communication, its integration into small diameter catheters is straightforward. Unlike ultrasound, no electronic ultrasonic transducer is required at the distal end of the cytoscope because light can be transmitted bidirectionally through optical fibers which are small and flexible. Moreover, since OCT uses light rather than sound, imaging is possible through air and does not require a transducing medium or direct contact with the tissue surface. In future animal studies, a recently developed OCT imaging endoscope<sup>12</sup> will be used for performing OCT imaging of in vivo urologic tissues.

Other modifications, which will likely improve the performance of OCT, will focus on alterations in source wavelength and bandwidth. Both penetration and contrast in OCT images are dependent on the wavelength of the incident source. It has recently been demonstrated that imaging at 1300 nm allows a dramatic increase in penetration compared with 800 nm.<sup>5</sup> Examination of other wavelengths in the near infrared could yield further improvements in both penetration and contrast. Furthermore, the resolution of the OCT system is dependent on the bandwidth of the source. Recently, broad bandwidth, short pulse femtosecond laser sources have been shown to yield resolution in the range of 2 to 4  $\mu\text{m}$ .<sup>11</sup> Light sources with these broad bandwidth characteristics have the potential to provide the clinician with cellular level resolution.

In conclusion, we have demonstrated high resolution, cross-sectional OCT imaging of several different urologic tissues in vitro and have correlated these images with conventional histopathology. The images acquired in this study provide information on tissue microstructure that could only previously be obtained with conventional biopsy. These results demonstrate that OCT may become a powerful diagnostic technology during urologic procedures, particularly the guidance of prostatic resection, suggesting that future in vivo investigations are merited.

*Acknowledgments.* The contributions of E. A. Swanson of MIT Lincoln Laboratory are greatly appreciated. We also would like to thank J. Gamba and J. Taralli for their technical support.

#### REFERENCES

1. Hanbury, D. C. and Sethia, K. K.: Erectile function following transurethral prostatectomy. *Br. J. Urol.*, **75**: 12, 1995.

2. Huang, D., Swanson, E. A., Lin, C. P., Schuman, J. S., Stinson, W. G., Chang, W., Hee, M. R., Flotte, T., Gregory, K., Puliafito, C. A. and Fujimoto, J. G.: Optical coherence tomography. *Science*, **254**: 1178, 1991.
3. Hee, M. R., Izatt, J. A., Swanson, E. A., Huang, D., Lin, C. P., Schuman, J. S., Puliafito, C. A. and Fujimoto, J. G.: Optical coherence tomography of the human retina. *Arch. Ophthalmol.*, **113**: 325, 1995.
4. Puliafito, C. A., Hee, M. R., Lin, C. P., Reichel, E., Schuman, J. S., Duker, J. S., Izatt, J. A., Swanson, E. A. and Fujimoto, J. G.: Imaging of macular diseases with optical coherence tomography. *Ophthalmol.*, **102**: 217, 1995.
5. Fujimoto, J. G., Brezinski, M. E., Tearney, G. J., Boppart, S. A., Bouma, B., Hee, M. R., Southern, J. F. and Swanson, E. A.: Biomedical imaging and optical biopsy using optical coherence tomography. *Nature Medicine*, **1**: 970, 1995.
6. Schmitt, J. M., Knuttel, A., Yablowsky, M. and Eckhaus, M. A.: Optical-coherence tomography of a dense tissue: statistics of attenuation and backscattering. *Physics in Medicine and Biology*, **39**: 1705, 1994.
7. Sergeev, A., Gelikonov, V., Gelikonov, G., Feldchtein, F., Pravdenko, K., Kuranov, R., Gladkova, N., Pochinko, V., Petrova, G. and Nikulin, N.: High-spatial-resolution optical-coherence tomography of human skin and mucous membranes. Conference on Lasers and Electro Optics '95, paper CThN4, Optical Society of America, 1995.
8. Brezinski, M. E., Tearney, G. J., Bouma, B. E., Izatt, J. A., Hee, M. R., Swanson, E. A., Southern, J. F. and Fujimoto, J. G.: Optical coherence tomography for optical biopsy: properties and demonstration of vascular pathology. *Circulation*, **93**: 1206, 1996.
9. Swanson, E. A., Huang, D., Hee, M. R., Fujimoto, J. G., Lin, C. P. and Puliafito, C. A.: High-speed optical coherence domain reflectometry. *Opt. Lett.*, **17**: 151, 1992.
10. Clivaz, X., Marquis-Weible, F. and Salathe, R. P.: High-resolution reflectometry in biological tissues. *Opt. Lett.*, **17**: 4, 1992.
11. Bouma, B., Tearney, G. J., Boppart, S. A., Hee, M. R., Brezinski, M. E. and Fujimoto, J. G.: High resolution optical coherence tomographic imaging using a mode-locked Ti:Al<sub>2</sub>O<sub>3</sub> laser source. *Opt. Lett.*, **20**: 1486, 1995.
12. Tearney, G. J., Boppart, S. B., Bouma, B. E., Brezinski, M. E., Weissman, N., Southern, J. F. and Fujimoto, J. G.: Scanning single mode fiber optic catheter-endoscope for optical coherence tomography. *Opt. Lett.*, **21**: 543, 1996.
13. Tearney, G. J., Bouma, B. E., Boppart, S. B., Golubovic, B., Swanson, E. A. and Fujimoto, J. G.: Rapid acquisition of in vivo biological images using optical coherence tomography. *Opt. Lett.*, **21**: 1408, 1996.
14. Charschan, S.: American National Standard for Safe Use of Lasers. American National Standards Institute (ANSI). Laser Institute of America, Orlando, FL, 1993.
15. Goldberg, B. B. and Liu, J.: Endoluminal urologic ultrasound. *Scan J. Urol. Nephrol. Suppl.*, **137**: 147, 1991.
16. Chancellor, M. B., Liu, J., Rivas, D. A., Karasick, S., Bagley, D. H. and Goldberg, B. B.: Intraoperative endo-luminal ultrasound evaluation of urethral diverticula. *J. Urol.*, **153**: 72, 1995.
17. Koraitim, M., Kamal, B., Metwalli, N. and Zaky, Y.: Transurethral ultrasonographic assessment of bladder carcinoma: its value and limitation. *J. Urol.*, **154**: 375, 1995.
18. Kirschner-Hermanns, R., Klein, H. M., Muller, U., Schafer, W. and Jaske, G.: Intraurethral ultrasound in women with stress incontinence. *Br. J. Urol.*, **74**: 315, 1994.
19. Goldberg, B. B., Bagley, D., Liu, J., Merton, D. A., Alexander, A. and Kurtz, A. B.: Endoluminal sonography of the urinary tract: preliminary observations. *AJR*, **156**: 99, 1991.